Synchronous regimes in ensembles of coupled Bonhoeffer–van der Pol oscillators

Alexey K. Kryukov,[1] Grigory V. Osipov,[1] Andrey V. Polovinkin,[2] and Jürgen Kurths[3,4]
[1]*Department of Calculational Mathematics and Cybernetics, Nizhny Novgorod State University, 23 Gagarin Avenue, 603950 Nizhny Novgorod, Russia*
[2]*Department of Radiophysics, Nizhny Novgorod State University, 23 Gagarin Avenue, 603950 Nizhny Novgorod, Russia*
[3]*Department of Physics, Humboldt University, 15, Newtonstrasse, 12489 Berlin, Germany*
[4]*Potsdam Institute for Climate Impact Research, A 31, Telegraphenberg, 14473 Potsdam, Germany*
(Received 20 June 2008; revised manuscript received 9 January 2009; published 7 April 2009)

We study synchronous behavior in ensembles of locally coupled nonidentical Bonhoeffer–van der Pol oscillators. We show that, in a chain of N elements not less than 2^{N-1}, different coexisting regimes of global synchronization are possible, and we investigate wave-induced synchronous regimes in a chain and in a lattice of coupled nonidentical Bonhoeffer–van der Pol oscillators.

DOI: 10.1103/PhysRevE.79.046209 PACS number(s): 05.45.Xt

I. INTRODUCTION

The understanding of human neuronal system functioning principles and information processing algorithms in neuron systems is an important actual challenge. Answers to these problems will have an immediate impact on the creation of highly efficient and low cost artificial neuron systems which are capable of solving tasks, apparent now as extremely complex [1,2]. There are already first solutions in this direction demonstrating the potentials of artificial networks constructed by analogy with neuron systems. For example, the processing of threads of multimedia data, including tasks of recognition of texts and images, optimum management of complex structures, brain-machine interactions, etc. [3–6].

The system of coupled Bonhoeffer–van der Pol oscillators (also known as FitzHugh-Nagumo elements) is one of the fundamental models in nonlinear dynamics and one of the most important models of neuroscience. In neuroscience there are only a few systems demonstrating more or less realistic simulation results, and manual understanding of what is happening and why it is happening in the media. The Bonhoeffer–van der Pol model is one of them. There are some more realistic models (e.g., well-known Huber-Braun [7] or Komendantov [8] models in neuroscience) but such systems have very complex dynamics, which is hard to understand and analyze. Even phase spaces for these systems are four dimensional. Also very often the Bonhoeffer–van der Pol model is some kind of bridge between observations of some effects at natural experiments or realistic model simulation, and understanding/analyzing of such results.

One basic feature of ensembles of neurons in the central and peripheral nervous systems, or in cardiac tissue is their ability to synchronize [1,2,9,10]. Therefore, the study of synchronization in chains and networks of elements simulating self-oscillatory activity of neurons and cardiac cells is extremely important. Actually, effect of multistability, i.e., coexistence of multiple attractors in phase space, was observed in different systems, not limited to cardiac cells or neurons: these are electromagnetical [11], mechanical [12], and biological [13] systems. In this paper we investigate synchronization in small (two and three elements) and rather large (chain) ensembles of coupled neuronlike oscillators. We demonstrate that such ensembles generate multistable synchronous regimes. In dependence on the initial conditions in a chain of N coupled oscillators, not less than 2^{N-1} different stable synchronous regimes are possible. For $N=2$ the existence of in-phase and antiphase regimes is proved analytically. Numerical simulations show the appearance of eight different synchronous regimes for $N=4$. In large ensembles different regimes of global and cluster synchronization are found.

II. MODEL

In this paper we investigate a chain of locally diffusively coupled Bonhoeffer–van der Pol (BvdP) oscillators as a model of a neuron network [14]:

$$\dot{x}_j = F_j(x_j, y_j) + d(x_{j+1} - 2x_j + x_{j-1}),$$

$$\dot{y}_j = G_j(x_j), \tag{1}$$

$$j = 1, \ldots, N,$$

where $F_j(x_j,y_j)=x_j-x_j^3/3-y_j$, $G_j(x_j)=\varepsilon(x_j+a_j)$, N is the number of elements in the chain, and d is the coupling between the elements, $\varepsilon \ll 1$, $0<a_j<1$. We consider slightly nonidentical oscillators with the nonidentity parameter $\Delta_{i,j}=a_i-a_j$. In different experiments free-end and periodical boundary conditions are taken. All motions in Eq. (1) can be divided in slow and fast motions because $\varepsilon \ll 1$ is very small. From a physiological point of view, the fast variable x can be considered as a voltage, and the slow variable y as a gating or recovery variable. Therefore, the cooperative behavior of neuronal networks or cardiac tissue can be at least qualitatively reproduced by a model of coupled BvdP oscillators. This oscillator was successfully used as individual cell for modeling the frequency entrainment of heart pacemakers [15]. Collective dynamics of synaptically coupled BvdP neurons was studied in [16].

For a single element:

$$\dot{x} = x - y - \frac{x^3}{3},$$

$$\dot{y} = \varepsilon(x + a). \tag{2}$$

There is one unstable steady state $(\bar{x},\bar{y})=(-a,\frac{a^3}{3}-a)$. It is (i) a focus if $a>\sqrt{1-2\sqrt{\varepsilon}}$, and (ii) a node if $a<\sqrt{1-2\sqrt{\varepsilon}}$. There

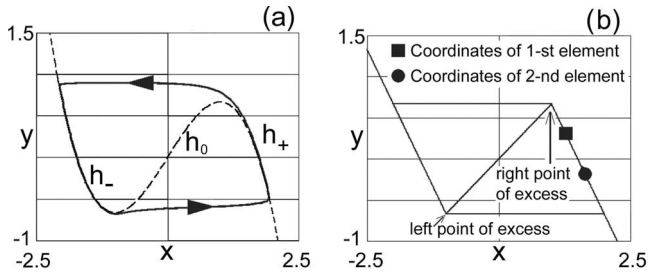

FIG. 1. (a) Phase portrait of system [Eq. (2)]. Dashed line is the curve of slow motions while solid line with arrows is the limit cycle. (b) In-phase regime at piecewise-linear approximation of the functions $F_{1,2}$ given according to [Eq. (4)].

exists also a stable limit cycle. It consists of fast and slow parts because of the smallness of ε. A typical phase portrait is shown in Fig. 1(a). Here $h_-(x)$ and $h_+(x)$ are the left and right steady parts, and $h_0(x)$ is the unstable part of the curve of slow motions.

III. TWO COUPLED NEURONS

Next we study a pair of coupled elements:

$$\dot{x}_1 = F_1(x_1,y_1) + d(x_2 - x_1),$$

$$\dot{y}_1 = G_1(x_1),$$

$$\dot{x}_2 = F_2(x_2,y_2) + d(x_1 - x_2),$$

$$\dot{y}_2 = G_2(x_2). \tag{3}$$

For some fixed parameters there are two limit cycles [9]. These cycles correspond to *in-phase* and *antiphase* synchronous regimes. For the analytical proof of this fact for $a_1 \approx a_2$, we consider a piecewise-linear approximation of the functions $F_{1,2}$ [Fig. 1(b)]:

$$F_i = \begin{cases} \dfrac{-4}{3}x_i - 2 - y_i, & \text{for } x_i \le -1 \\ \dfrac{2}{3}x_i - y_i, & \text{for } -1 < x_i < 1 \\ \dfrac{-4}{3}x_i + 2 - y_i, & \text{for } x_i \ge 1. \end{cases} \tag{4}$$

These functions have two extrema: the right extreme $y_{1,2} = 2/3 + d(x_{2,1} - x_{1,2})$, and the left extreme $y_{1,2} = -2/3 + d(x_{2,1} - x_{1,2})$. Under the general assumption that the switching time from $h_\pm(x)$ to $h_\mp(x)$ is extremely small, in the steady regime there are four possible types of mutual arrangements of phase points of both elements: (i) both are situated in $h_+(x)$; (ii) both are situated in $h_-(x)$; (iii) the phase point of the first element is situated in $h_+(x)$, and the phase point of the second element is situated in $h_-(x)$; (iv) the phase point of the first element is situated in $h_-(x)$, and the phase point of the second element is situated in $h_+(x)$.

We consider elements to be synchronized in phase if $t_{isi} \equiv t_2 - t_1 \ll T$, where t_j is the moment of switching from the passive phase to the active one at the jth element, and T is the period of synchronous regime. If $t_{isi} \equiv t_2 - t_1 \sim T/2$, we consider elements to be synchronized in antiphase. Note that for $a_1 = a_2$ for an in-phase regime $x_1 = x_2$, $y_1 = y_2$, and for an antiphase regime the lag between two time series is equal to $T/2$.

Let us study the first case: both elements are on $h_+(x)$ [see Fig. 1(b)]. After substitution $\tau = \varepsilon t$ at vanishing ε, according to Eq. (4) we get the simplified model:

$$0 = F_1(x_1,y_1) + d(x_2 - x_1),$$

$$\frac{dy_1}{d\tau} = x_1 + a_1,$$

$$0 = F_2(x_2,y_2) + d(x_1 - x_2),$$

$$\frac{dy_2}{d\tau} = x_2 + a_2. \tag{5}$$

Solving this linear system, we find both limit cycles. To do this, we build the mapping $df_{n+1}(df_n)$, where n corresponds to the nth passing of the limit cycle, and $df_n = y_1^n - y_2^n$. Without loosing generality, let us consider the following case. Let y_1^n, y_2^n be the values of y_1 and y_2 on the nth passing of the limit cycle. Then the first element just comes to the line $h_-(x)$. The state y_2^n of the second element can be arbitrary on the lines $h_-(x)$ or $h_+(x)$. The state y_1^n of the first element is defined through y_2^n. Let us assume that the second element is located on the $h_+(x)$. Then

$$y_1^n = 2/3 + d(x_2 - x_1) = \hat{d}^{-1}(4\bar{d}/3 - dy_2^n), \tag{6}$$

where $\bar{d} = 2/3 + d$ and $\hat{d} = 4/3 + d$.

For the moment let $\tau = t_1$, in which the second element jumps to the line $h_-(x)$. Then, solving system (5), one obtains for $y_1(t_1)$ and $y_2(t_1)$:

$$y_1^{-+}(t_1) = \left[\frac{1}{2}(y_1^n - y_2^n) + 2 - (a_1 - a_2)\bar{d}\right]\exp\left(-\frac{t_1}{2\bar{d}}\right) + \left[\frac{1}{2}(y_1^n + y_2^n) - \frac{2}{3}(a_1 + a_2)\right]\exp\left(-\frac{3t_1}{4}\right) - 2 - da_2 + \hat{d}a_1, \tag{7}$$

$$y_2^{-+}(t_1) = \left[\frac{1}{2}(y_2^n - y_1^n) - 2 + (a_1 - a_2)\bar{d}\right]\exp\left(-\frac{t_1}{2\bar{d}}\right) + \left[\frac{1}{2}(y_1^n - y_2^n) - \frac{2}{3}(a_1 + a_2)\right]\exp\left(-\frac{3t_1}{4}\right) + 2 - da_2 + \hat{d}a_1. \tag{8}$$

In Eqs. (7) and (8) the index "−+" means that the first element is on the line $h_-(x)$, and the second one is on the line $h_+(x)$. From another side, because of the fact that at $\tau = t_1$ the second element jumps to the line $h_-(x)$, we have

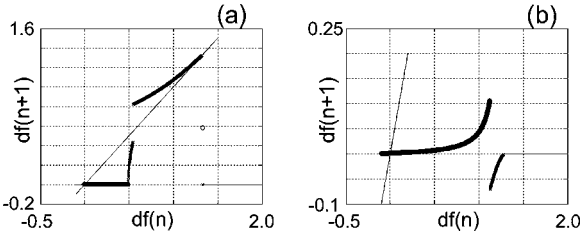

FIG. 2. Map $df_{n+1}(df_n)$. Initially the second element is located on $h_-(x)$. The parameters are $a_1=0.995$, $a_2=0.994$, $\varepsilon=0.02$, and (a) $d=0.002$ and (b) $d=0.05$.

$$y_2(t_1) = \frac{2}{3} + \frac{d}{2\bar{d}}[y_2(t_1) - y_1(t_1) - 4]. \tag{9}$$

Comparing Eqs. (8) and (9) and taking into account Eq. (7), we can find the moment t_1. Now both elements are on the line $h_-(x)$. The respective values $y_1(\tau)$ and $y_2(\tau)$ can be calculated:

$$y_1^{--}(\tau) = \left\{\frac{1}{2}[y_1(\tau_0) - y_2(\tau_0)] - (a_1 - a_2)\bar{d}\right\}\exp\left(-\frac{\tau - \tau_0}{2\bar{d}}\right) + \left\{\frac{1}{2}[y_1(\tau_0) + y_2(\tau_0)] + 2 - \frac{2}{3}(a_1 + a_2)\right\} \times \exp\left[-\frac{3}{4}(\tau - \tau_0)\right] - 2 - da_2 + \hat{d}a_1, \tag{10}$$

$$y_2^{--}(\tau) = \left\{\frac{1}{2}[y_2(\tau_0) - y_1(\tau_0)] + (a_1 - a_2)\bar{d}\right\}\exp\left(-\frac{\tau - \tau_0}{2\bar{d}}\right) + \left\{\frac{1}{2}[y_1(\tau_0) + y_2(\tau_0)] + 2 - \frac{2}{3}(a_1 + a_2)\right\} \times \exp\left[-\frac{3}{4}(\tau - \tau_0)\right] - 2 - da_1 + \hat{d}a_2, \tag{11}$$

Each element can reach the left extreme before the other element. This depends on the initial conditions and the parameters. At $\tau=t_2$ one of the elements reaches the left extreme. Then $y_1(t_2)$ and $y_2(t_2)$ can be obtained from Eqs. (10) and (11). From another side, we can use the fact that one element at $\tau=t_2$ is located in the left extreme. Therefore, we can define the moment t_2. If we move further along the cycle, then we can obtain (i) the moment where the first element jumps again from the line $h_+(x)$ to the line $h_-(x)$, and (ii) the values y_1^{n+1} and y_2^{n+1}. Therefore, we can build the mapping $df_{n+1}(df_n)$. This mapping at $d=0.002$, $a_1=0.995$, and $a_2=0.994$, and at the initial state of the second element the $h_-(x)$ is presented in Fig. 2(a). It is visible that there are two steady fixed points of this map, each related to a certain synchronous regime. The fixed point in the vicinity of zero corresponds to an in-phase regime ($x_1 \approx x_2$) and the point near $df(n)=1.323$ corresponds to an antiphase regime. Both of these regimes appear if the coupling strength d becomes larger than some critical value. With further increase in d, the fixed point corresponding to the antiphase regime disappears but the fixed point corresponding to the in-phase regime remains [Fig. 2(b)]. This means that for relatively large coupling only an in-phase synchronous regime exists.

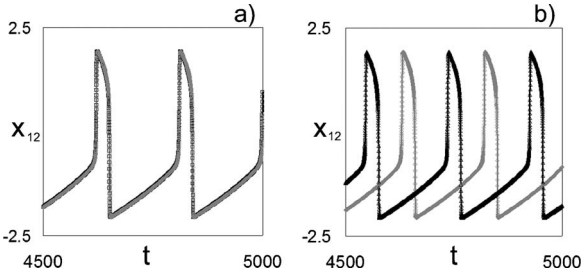

FIG. 3. Time series for (a) in-phase and (b) antiphase regimes of system [Eq. (1)] for $N=2$, $\varepsilon=0.02$, $a_1=0.995$, and $a_2=0.994$. Black dots correspond to time series of the first element, and gray dots correspond to time series of the second element.

These analytical results obtained for a linear approximation of the functions $F_{1,2}$ are tested in numerical experiments with original model (3) for $\varepsilon=0.02$. This way we get the existence of in-phase and antiphase synchronous regimes. The appropriate time series are given in Figs. 3(a) and 3(b). It is important to note that the antiphase regime is realized not only in some intervals of the coupling parameter d but in some interval of the nonidentity parameter $\Delta_{1,2}=a_1-a_2$ as well. In the case of a large $\Delta_{1,2}$, when even for one of the elements the time of movement along $h_+(x)$ is close to the time of movement along $h_-(x)$, the antiphase regime disappears. Therefore, it is possible to assume that the strong difference between the times of two parts of slow movement is a reason for the existence of two (and very big for large ensembles) synchronous regimes. We have also calculated the evolution of the observed frequencies $\omega_j=2\pi/T_j$ vs the parameter d. Here $T_j=1/M\,\Sigma_{i=1}^{M}T_{ij}$, where $M\to\infty$, $j=1,2$, and T_{ij} is the sequence of time intervals between consecutive maxima of the realization $x_j(t)$. In other words ω_j is an averaged frequency of the occurrence of maxima in the time series $x_j(t)$.

As our numerical experiments show, the in-phase and antiphase regimes have strongly different observed frequencies ω. The frequency of the in-phase regime is close to the maximal of the individual frequencies of the uncoupled elements. The fastest element is the source of the synchronous oscillations. It sets rhythm to others and can be called "pacemaker." The frequency of the antiphase regime goes to zero if d increases, and therefore, the antiphase regime disappears (Fig. 4). It can be noticed that for identical elements the decreasing of this frequency can be estimated analytically. Thus, at $d>d_{cr}$ only the in-phase regime exists.

The simplified model [Eq. (5)] reproduces most considered effects, which take place in a pair of coupled oscillators: (i) the frequency of the in-phase regime is close to the maximal individual frequency among elements and does not strongly depends on coupling; (ii) the frequency of the antiphase regime at rather low coupling is close to the minimal individual frequency among elements; (iii) at high coupling only in-phase regime exists.

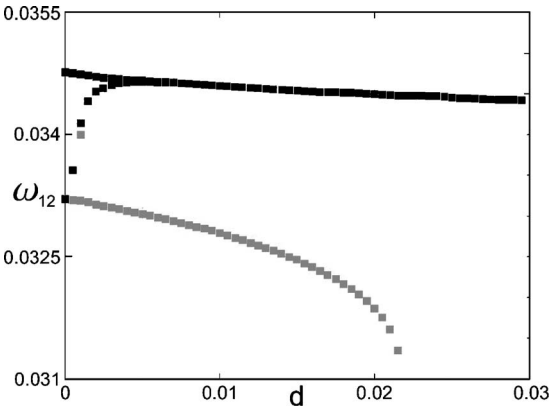

FIG. 4. Synchronization regimes in two coupled elements. Distribution of mean frequencies vs coupling. The parameters are $\varepsilon=0.02$, $a_1=0.995$, and $a_2=0.994$. Black dots correspond to experiments with in-phase initial conditions, and gray dots correspond to experiments with antiphase initial conditions.

IV. SYNCHRONOUS REGIMES ORIGINATION AND DESTRUCTION IN TWO COUPLED ELEMENTS

In this section we consider dynamical regimes changing in a pair of coupled elements at different nonidentity $\Delta_{1,2}$ and coupling d. The respective bifurcation diagram is shown in Fig. 5. For some value of $\Delta_{1,2}$ if $d<d^1_{\min}$ (area 1 in Fig. 5) phase beating can be observed, i.e., time shifts between the maxima of x_1 and x_2 or y_1 and y_2 are permanently changing from zero up to some value.

A detailed analysis based on Poincare maps and Lyapunov characteristic exponent calculations exhibits very complex chaotic regimes in the system at $d<d^1_{\min}$. At d near but less than $d^1_{\min}$, the frequency of the phase beating decreases and at $d=d^1_{\min}$ the stable limit cycle, corresponding to an antiphase synchronous regime, appears through the value of the limit cycle multiplier $s=+1$ bifurcation. Note that for $0<d^1_{\min}-d\ll 1$ both elements oscillate in a regime, close to an antiphase most part of time, and a few time elements oscillate in regime, close to an in-phase.

At increasing d up to $d=d^2_{\min}$ the stable limit cycle, corresponding to an in-phase synchronous regime, originates through the value of the limit cycle multiplier $s=+1$ bifurcation. Thus, multistability of synchronous regimes exists in area 3 in Fig. 5.

At $d=d_{\max}$, the stable limit cycle of the antiphase regime disappears and only an in-phase synchronous regime exists in area 4 in Fig. 5. The scenario of antiphase regime destruction could be different, depending on the element nonidentity: through the value of the limit cycle multiplier $s=+1$ or $s=-1$ (period-doubling) bifurcations. But from the point of multistability of the synchronous regimes, scenario of this bifurcation is not important because phase trajectories of the cycle after period-doubling bifurcation lie in the vicinity of the antiphase limit cycle before the period-doubling bifurcation. It is noteworthy that dependencies of $d^2_{\min}(\Delta_{1,2})$ and $d^2_{\min}(\Delta_{1,2})$ on the $(d,\Delta_{1,2})$ plane are close to be in direct proportion, and $d_{\max}(\Delta_{1,2})$ is nonlinear.

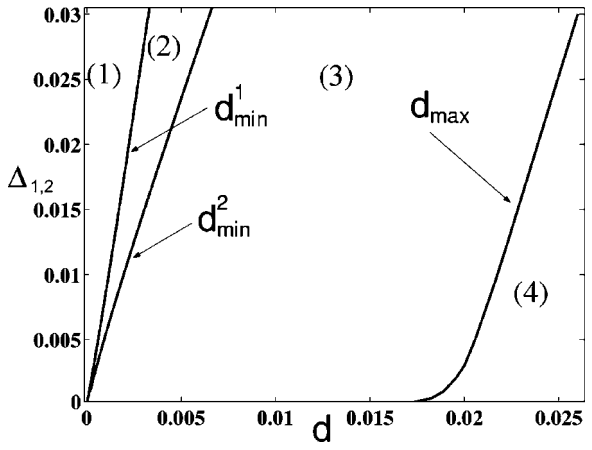

FIG. 5. Bifurcation diagram of synchronous regimes in system (3) on $(d,\Delta_{1,2})$. (1) Phase beating area, (2) monostability of the antiphase synchronous regime, (3) multistability of the in-phase and the antiphase synchronous regimes, and (4) monostability of the in-phase synchronous regime. Bifurcation curves $d^1_{\min}(\Delta_{1,2})$, $d^2_{\min}(\Delta_{1,2})$, and $d_{\max}(\Delta_{1,2})$.

V. THREE COUPLED ELEMENTS

In an ensemble of three coupled elements

$$\dot{x}_1 = F_1(x_1,y_1) + d(x_2 - x_1),$$

$$\dot{y}_1 = G_1(x_1),$$

$$\dot{x}_2 = F_2(x_2,y_2) + d(x_3 - 2x_2 + x_1),$$

$$\dot{y}_2 = G_2(x_2),$$

$$\dot{x}_3 = F_3(x_3,y_3) + d(x_2 - x_3),$$

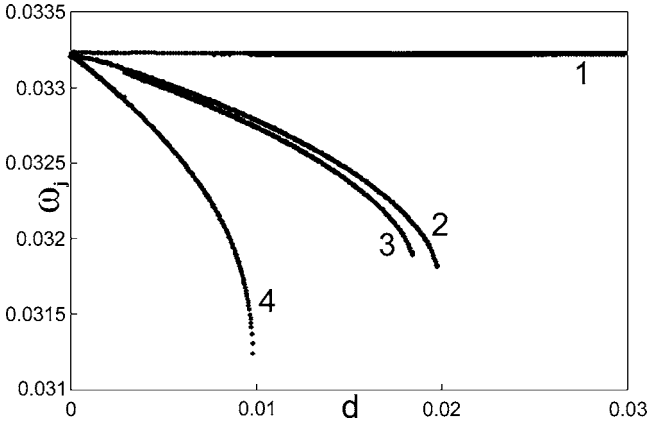

FIG. 6. Synchronization regimes in three coupled elements. Distribution of mean frequencies $\omega_{1,2,3}$ vs coupling. Curve 1 corresponds to an in-phase synchronous regime (i). Curve 4 - to an antiphase synchronous regime (ii). Curve 2 - to a mixed regime (iii). Curve 3 - to a mixed regime (iv). The parameters are: $\varepsilon=0.02$, $a_1=0.995$, $a_2=0.994\,93$, $a_3=0.994\,86$.

$$\dot{y}_3 = G_3(x_3), \tag{12}$$

the following synchronous regimes were found: (i) in-phase regime ($x_1 \approx x_2 \approx x_3, y_1 \approx y_2 \approx y_3$); (ii) antiphase regime (there is no pair of elements, synchronized in in-phase); (iii) regime, for which the first and the second elements are synchronized in in-phase, and the second and the third in antiphase; (iv) regime, for which the first and the second elements are synchronized in antiphase, and the second and the third in in-phase.

In some sense regimes (iii) and (iv) can be called mixed regimes. Therefore $2^{N-1}=2^2=4$ different synchronous regimes are possible. The lags between the time series $x_1(t), x_2(t), x_3(t)$ are not constant and can be changed in dependence on the parameters. Under some conditions the regime of splay state occurs, for which the time between the maxima of the time series is close to $T/3$, where T is the period of the synchronous oscillations.

The dependence of the observed frequencies on the coupling of the three elements is shown in Fig. 6. Each curve in the figure describes this dependence at one of the four regimes of global synchronization. One can observe existence of the coupling interval, where all four regimes are stable.

The mixed regimes are established at some frequency ω^s_{mix}, such that $\omega^s_{\text{anti}} < \omega^s_{\text{mix}} < \omega^s_{\text{in}}$, where $\omega^s_{\text{anti}}, \omega^s_{\text{in}}$ are the synchronization frequencies of the antiphase and the in-phase synchronous regimes, respectively. Mixed regimes exist in a wider interval of d than the antiphase regime. With increasing d, the mixed regimes disappear, and only the in-phase regime remains.

VI. FOUR COUPLED ELEMENTS

Let us suppose that in the chain of L elements M synchronous regimes coexist. Adding a new element to the chain, this new element can be synchronized in in-phase and in antiphase to its neighbor. M regimes coexist in the in-phase case, and M regimes coexist in the antiphase case; hence totally, $2M$ synchronous regimes coexist. Thus, two synchronous regimes coexist in a pair of coupled oscillators, and adding a new element to the chain doubles the number of synchronous regimes. But experiments with two and three elements are not very convincing here.

Therefore, we consider an ensemble of four elements with linearly distributed parameters a_j ($\Delta_{j,j+1}=\Delta$). Finding eight stable synchronous regimes in such systems will give us more confidence in the assumption that 2^{N-1} different regimes of global synchronization are possible in a chain of N elements at the same values of parameters. Obtaining and analyzing regimes, e.g., $N=6$ or $N=8$ ($2^{8-1}=128$ regimes for

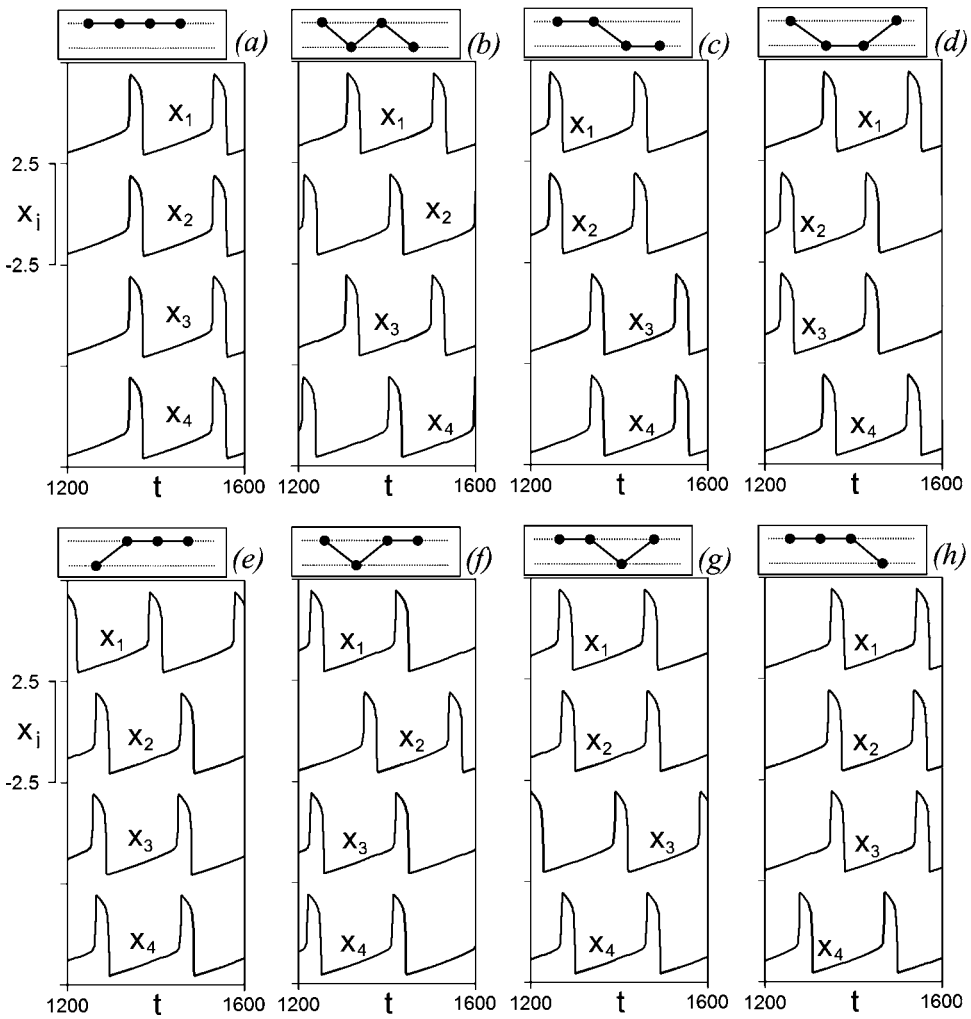

FIG. 7. Eight stable synchronous regimes in four coupled elements: (a) in-phase regime $\Omega_a=0.033\,131$; (b) antiphase regime $\Omega_b=0.032\,255$; (c)–(h) mixed regimes: $\Omega_c=0.032\,740$, $\Omega_d=0.032\,744$, $\Omega_e=0.032\,583$, $\Omega_f=0.032\,613$, $\Omega_g=0.032\,633$, and $\Omega_h=0.032\,661$. The parameters are $\varepsilon=0.02$, $a_1=0.995$, $\Delta=0.000\,07$, $d=0.0055$, periodical boundary conditions were used.

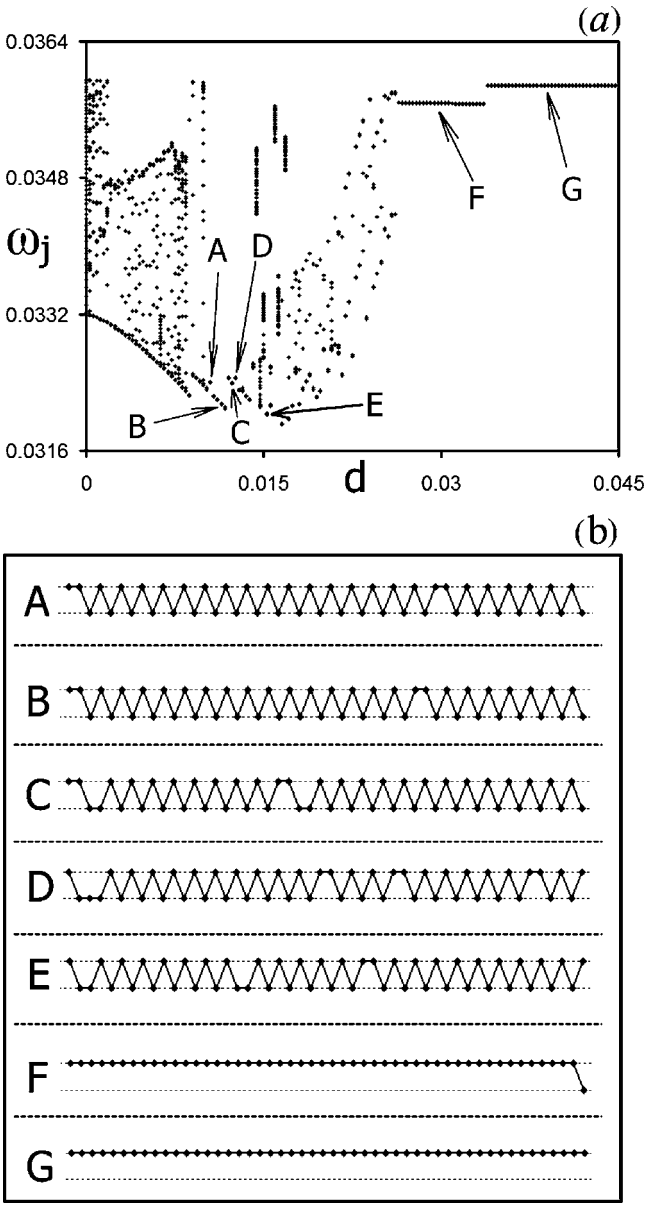

FIG. 8. (a) Synchronization frequencies in a chain of 50 coupled elements for $a_1=0.995$, $\Delta=0.000\,45$, and $\varepsilon=0.02$. We used free boundary conditions and saw-tooth initial conditions. *A*, *B*, *C*, *D*, *E*, *F*, *G*—examples of different synchronous regimes in the chain; (b) schematic sketch of synchronous regimes explored.

$N=8$) have no principal difference comparing with $N=4$. In experiments with four coupled cells we have indeed found all eight synchronous regimes (see Fig. 7) at the same values of parameters.

VII. GLOBAL AND CLUSTER SYNCHRONIZATIONS IN LARGE ENSEMBLES

The results obtained in previous sections allow us to expect that in a chain of N elements for some parameters 2^{N-1} different regimes of global synchronization are possible. In order to study synchronization phenomena in rather large ensembles of neuronlike elements, we investigate a chain of 50 coupled oscillators with linearly distributed parameters a_j ($\Delta_{j,j+1}=\Delta$), which means a monotonous distribution of their individual frequencies. Arrays of oscillators with natural frequencies varying monotonously along them are interesting both conceptually and because they are encountered in a natural fashion in various situations [17]. Two rather illustrative examples are below. One of them concerns dynamics of a mammalian small intestine. If one isolates mammalian small intestine sections 1–3 cm long, then each of them will be able to oscillate at a definite frequency. Changes along the intestine may be regarded to be monotonous at rather long distances [18]. The other example is the vortex shedding in flow past cone-shaped bodies (e.g., supports or chimney stacks). Such research also involves the analysis of an array of coupled oscillators with monotonously varying natural frequencies if the derivative with respect to the coordinate along the cone axis is replaced by finite differences (see, e.g., [19]).

Each synchronous regime (except the in-phase one) has minimal and maximal values of coupling ($d_{\min}, d_{\max}$) of their stability. A detailed analysis of two coupled oscillators shows that $d_{\min}$ of the in-phase regime is higher than $d_{\min}$ for the antiphase regime. Moreover $d_{\max}$ of the antiphase regime has the minimal value among all other synchronous regimes. Thus, it is possible to assume that, at the interval of coupling between the minimal value of coupling of the in-phase synchronous regime $d_{\min}^{\text{in-phase}}$ and the maximal value of coupling of the antiphase regime $d_{\max}^{\text{anti-phase}} 2^{N-1}$ different synchronous regimes are stable.

In numerical experiments several of such regimes have been found (Fig. 8). The evolution of the synchronization frequencies for an increasing coupling parameter is similar to the evolution in the systems of two and three coupled elements. As in the previous computations, in the in-phase regime the synchronization frequency is close to the maximal of the individual frequencies. This regime remains with increasing d.

Another interesting finding we have observed in the chain of 128 elements with randomly distributed parameter a and periodic boundary conditions is that we have obtained a synchronous regime having a higher frequency than the in-phase regime. This regime exists due to a wave of excitation propagating in the chain ("wave-induced regime"). The frequency of this regime is conditioned by the speed of the wave and the length of the chain. This regime exists only if its frequency is higher than the frequency of the fastest element of the chain. Typical spatiotemporal diagrams of the in-phase

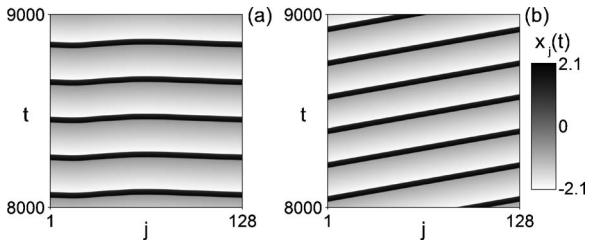

FIG. 9. Time series of the (a) in-phase and (b) wave-induced regimes in a chain of 128 elements with periodic boundary conditions, a_j is distributed randomly in the interval (0.9968, 0.9975).

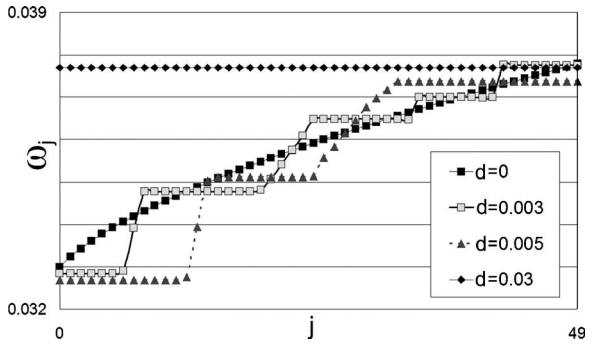

FIG. 10. Global ($d=0.03$) and cluster synchronizations in a chain of 50 coupled elements for $a_1=0.995$, $\Delta=0.001$, and $\varepsilon=0.02$.

and wave regime are shown in Fig. 9, respectively.

Therefore, the in-phase and the wave-induced synchronous regimes are conditioned, respectively, by: (i) the fastest element, which sets rhythm of oscillations to all other cells in the chain. Frequency of the in-phase synchronous regime is close to the individual frequency of this element. (ii) The pulse propagating through the chain and activating elements sequentially. Synchronization frequency of this regime is conditioned by the size of the chain and the propagation velocity, which is determined by coupling and individual cells' parameters. If frequency of the wave-induced regime becomes lower than the frequency of the fastest element, the wave-induced regime will disappear.

With an increase in coupling from zero the formation of groups of synchronized neighboring elements, i.e., clusters of synchronization, appears. Effect of cluster synchronization can be observed in different models, e.g., in-phase oscillators [20]. But as the rotation frequencies are constant in [20], global synchronization establishes at some average frequency among individual frequencies of the elements. We consider relaxational oscillators; hence, the in-phase synchronization establishes at frequency, which is close to the individual frequency of the fastest element in the chain. The number of clusters decreases with increasing d, and in the chain of 50 coupled elements for $d \geq 0.03$ global synchronization sets in (Fig. 10). Note that the formation of synchronous clusters is observed for randomly distributed parameters a_j as well [17].

VIII. SYNCHRONIZATION OF LATTICES BY SPIRAL AND TARGET WAVES

In the previous section it was shown that synchronization can be achieved due to excitation pulse, propagating through the chain. In case of lattice [two-dimensional (2D)] synchronization can be also achieved due to one-dimensional (1D) pulses, i.e., propagating through one dimension (in case of periodical boundary conditions). But existence of the second spatial dimension allows realizing spiral and target waves in the lattice, which like 1D pulses set common rhythm to all other elements.

In a lattice of 100×100 elements (free boundary conditions) two types of wave-induced regimes were obtained: (i) a regime, characterized by one target wave, propagating from the fastest element of the lattice, and (ii) a regime induced by existence of a spiral wave in the lattice. Typical snapshot $x_{ij}(t)$ of the system in the synchronous regime with one target wave propagation is shown in Fig. 11(a). The frequency of this regime is equal to the frequency of the fastest element of the chain. In some sense this regime can be called in-phase synchronous regime.

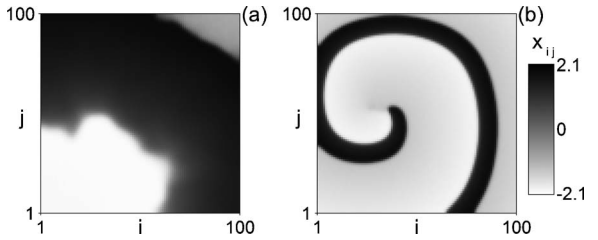

FIG. 11. Snapshot $x_{ij}(t)$ in a 100×100 lattice at the regime with: (a) one target wave, which sets the rhythm to the lattice, (b) one spiral wave, sets the rhythm to the lattice. Parameters: a_{ij} distributed randomly in the interval (0.975, 0.995), $d=0.4$, $\varepsilon=0.02$.

Typical snapshot $x_{ij}(t)$ of the system in the regime with existing of one spiral wave in the lattice is shown in Fig. 11(b). The spiral wave sets a rhythm to the lattice, which is higher than the frequency of the fastest element in the lattice.

IX. CONCLUSIONS

Based on the presented results it is possible to assume that, in a chain of N locally diffusively coupled Bonhoeffer–van der Pol oscillators with free boundary conditions for fixed values of parameters, the number of different global synchronous regimes can be not less than 2^{N-1}. This was numerically confirmed for $N=4$. An analytical proof for the existence of two synchronous regimes was performed for $N=2$. In large ensembles a transition to global synchronization is accomplished with the formation of synchronization clusters. In a chain with free boundary conditions for relatively strong coupling, only the in-phase synchronous regime exists, which is realized on a frequency close to the maximal of the individual frequencies. In this chain and in the lattice of Bonhoeffer–van der Pol oscillators, we investigated wave-induced regimes with rhythms set by the waves.

Many theoretical and experimental results show that synchronization phenomena play a very important role in brain activity. It is assumed that synchronous firing of neurons is an essential mechanism for information processing. Therefore, the observed multistability of synchronous regimes may be useful for understanding of mechanisms of different brain functions including image storage and recognition [5], visual perception [6], memory processing [21], control of movement [3], and posture [4].

ACKNOWLEDGMENTS

This work is done through financial support from RFBR Projects No. 08-02-92004 and No. 08-02-97049.

[1] E. Mosekilde, Yu. Maistrenko, and D. Postnov, *Chaotic Synchronization–Applications to Living Systems* (World Scientific, Singapore, 2002).
[2] P. Varona, J. J. Torres, R. Huerta, H. D. I. Abarbanel, and M. I. Rabinovich, Neural Networks **14**, 865 (2001).
[3] A. Beuter, J. G. Milton, C. Labrie, and L. Glass, *Proceedings of the 1989 IEEE International Conference on Systems, Man, and Cybernetics, Cambridge, MA, 1989* (IEEE, Los Alamitos, CA, 1989) p. 899.
[4] C. W. Eurich and J. G. Milton, Phys. Rev. E **54**, 6681 (1996).
[5] K. Macleod, A. Bäcker, and G. Laurent, Nature (London) **395**, 693 (1998).
[6] *Ambiguity in Mind and Nature*, edited by P. Kruse and M. Stadler (Springer-Verlag, New York, 1995).
[7] H. Braun, K. Voigt, and M. Huber, BioSystems **71**, 39 (2003).
[8] A. Komendantov and C. Canavier, J. Neurophysiol. **87**, 1526 (2002).
[9] G. V. Osipov, J. Kurths, and Ch. Zhou, *Synchronization in Oscillatory Networks* (Springer, Berlin, 2007).
[10] A. S. Pikovsky, M. G. Rosenblum, and J. Kurths, *Synchronization: A Universal Concept in Nonlinear Science* (Cambridge University Press, Cambridge, 2001).
[11] D. Dangoisse, P. Glorieux, and D. Hennequin, Phys. Rev. A **36**, 4775 (1987).
[12] J. M. T. Thompson and H. B. Stewart, *Nonlinear Dynamics and Chaos* (Wiley, Chichester, 1986).
[13] J. Foss, A. Longtin, B. Mensour, and J. Milton, Phys. Rev. Lett. **76**, 708 (1996).
[14] K. F. Bonhoeffer, Naturwiss. **40**, 301 (1953).
[15] V. Torre, J. Theor. Biol. **61**, 55 (1976).
[16] K. Tsumoto, T. Yoshinaga, and H. Kawakami, Phys. Rev. E **65**, 036230 (2002).
[17] G. V. Osipov and M. M. Sushchik, Phys. Rev. E **58**, 7198 (1998).
[18] N. E. Diamant, P. K. Rose, and E. J. Davidson, Am. J. Physiol. **219**, 1684 (1970).
[19] B. R. Noack, F. Ohle, and H. Eckelman, J. Fluid Mech. **227**, 293 (1991).
[20] H. Daido, Prog. Theor. Phys. **102**, 197 (1999).
[21] B. Mensour and A. Longtin, Phys. Lett. A **205**, 18 (1995).